ISSN No: 2348-4845
International Journal & Magazine of Engineering, Technology, Management and Research
A Peer Reviewed Open Access International Journal

Power Management in Distributed DC Grid Integrated To Hybrid Renewable Wind and Fuel Energy Conversion Systems

S. Vinitha
M.Tech (Energy Systems)
Department of Electrical Engineering
JBIET, Hyderabad,
Telangana, India.

K. Giribabu
Assistant Professor
Department of Electrical Engineering
JBIET, Hyderabad,
Telangana, India.

Fatima Azra
Associate Professor & HoD
Department of Electrical Engineering
JBIET, Hyderabad,
Telangana, India.

Abstract

This paper proposes an integrated wind and wave power generation system fed to an ac power grid or connected with an isolated load using a dc microgrid. A bidirectional dc/dc converter is proposed to achieve the integration of both wind and wave power generation systems with uncertainty and intermittent characteristics. The wind power generation system simulated by a permanent-magnet synchronous generator (PMSG) driven by a wind turbine (WT) is connected to the dc microgrid through a VSC of PMSG. The wave power generation system simulated by an LPMG driven by a linear permanent magnet motor (LPMM) is also connected to the dc microgrid through a VSC of LPMG. Classical wind energy conversion systems are usually passive generators. The generated power does not depend on the grid requirement but entirely on the fluctuant wind condition. A dc-coupled wind/hydrogen/super capacitor hybrid power system is studied in this paper. The purpose of the control system is to coordinate these different sources, particularly their power exchange, in order to make controllable the generated power. As a result, an active wind generator can be built to provide some ancillary services to the grid. The control system should be adapted to integrate the power management strategies. Two power management strategies are presented and compared experimentally.

INTRODUCTION

IN recent years, renewable energy and distributed generationsystems (DGSs) have attracted increasing attention and havebeen extensively researched and developed. The rise in several countries makes it possiblethat this kind of DGS can be practically applied to a grid-tiedsystem or an isolated system with wind power, solar energy, and hydropower. The output of DGS usually includes two kinds: dc and variable ac. Moreover, the generating capacity of DGScomparing with conventional large synchronous generators is much smaller, and hence, the dc micro grid can be practically applied to convert the generated time-varying quantities ofnatural renewable energy and DGS into smooth dc electricitythat can then be converted back into ac quantities delivered to other power systems.

Because of the intermittence of renewable energy and DGS, bidirectional dc/dc convertersare usually necessary to feed the connected loads with smoothpower. Super capacitors Super-capacitors, ultra-capacitors (commercialdenominations given originally by its manufactures NipponElectric Company, NEC, in Japan, and by PinnacleResearch Institute, PRI, in USA) or electrochemical doublelayercapacitor (EDLC, technical name) are devices thatcan be used as energy storage systems, that have highenergy and power densities, a high efficiency, nearly 95%and a large life expectancy.

A hybrid electric vehicular power systemutilizedtwo motors connected to a dc bus through a voltage-sourceconverter (VSC) and a bidirectional converter was connectedbetween a battery and the dc bus. The dynamic average modelwas used for all power electronics models by neglectingthe switching phenomena to reduce simulation computationalintensity.A non-isolated bidirectional zero-voltage switchingdc/dc converter was

ISSN No: 2348-4845
International Journal & Magazine of Engineering, Technology, Management and Research
A Peer Reviewed Open Access International Journal

proposed, and the converter utilized avery simple auxiliary circuit consisting of an additional windingof a main inductor and an auxiliary inductor to reach zerovoltageswitching and reduce the reverse-recovery problem of power diodes.

The proposed dc micro grid was also usedto supply sensitive electronic loads during ac grid outages inorder to offer uninterruptible power system protection. Toachieve power sharing and improve economic benefit, a dcbusvoltage control technique for parallel integrated permanentmagnetwind power generation systems was proposed, and the technique was based on a master–slave control tosolve controller discrepancy problems. A 12-kW experimental system was constructed to confirm the effectiveness of the proposed scheme.

Hybrid DC Grid Modeling

Fig. 1 shows the configuration of the studied integrated windand wave power generation system connected to an ac grid through a dcmicrogrid. The wind power generation system simulatedby a permanent-magnet synchronous generator (PMSG) driven by a wind turbine (WT) is connected to the dc microgridthrough a VSC of VSC_PMSG. The wave power generation system simulated by an LPMG driven by a linear permanentmagnetmotor (LPMM) is also connected to the dc microgridthrough a VSC of VSC_LPMG. A resistive dc load R_{oad} disconnected to the dc micro grid through a load dc/dc converter.

To achieve stable power flow (or power balance condition)and load demand control of the dc micro grid under different operating conditions, a battery is connected to the dc microgridthrough a bidirectional dc/dc converter, while an ac grid isconnected to the dc micro grid through a bidirectional grid-tiedinverter and a transmission line. When available wind powerand/or wave power can be injected into the dc micro grid with awfully charged battery, the surplus power of the dc micro grid cane delivered to the ac grid through the bidirectional grid-tiedinverter. When no wind power or no wave power is delivered to the dc micro grid with a low-energy battery, the insufficientpower of the dc micro grid can be captured from the ac gridthrough the bidirectional grid-tied inverter. The power of the resistive dc load R_{Load} can be obtained from the dc microgridthrough the load dc/dc converter only when the dc microgridhas enough power. The load dc/dc converter with the resistive load R_{Load} can also slightly adjust the power balancecondition of the dc micro grid. The control functions of the bidirectionaldc/dc converter, the bidirectional grid-tied inverter, and the load dc/dc converter must be adequately coordinatedwith each other to obtain stable operation of the dc micro grid.

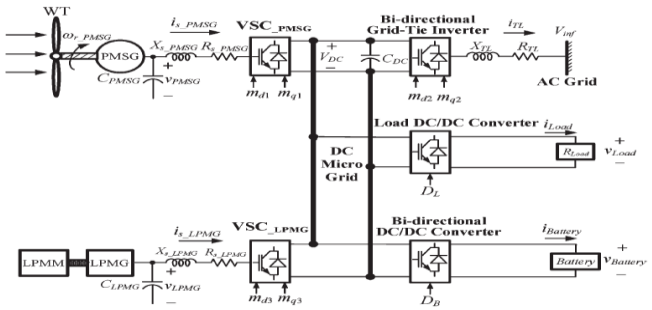

Fig 1: Configuration dc micro grid

System modeling

Wind turbine characteristic

A Wind Turbine (WT) cannot fully capture wind energy. Then, the output power of the wind-turbines described as

$$P_{turbine} = \frac{1}{2}\rho\pi R^2 C_p(\lambda,\beta)v^3$$

where, ρ is the air density (kg/m3), R is the blade radius (m), CP is the performance coefficient of theturbine which is a function of the pitch angle of rotor blades β (in degrees) and v is the wind speed (inm/s). The tip-speed ratio λ is given by:

$$\lambda = \frac{w_m R}{v}$$

Where R and w_m are the blade length (in m) and the wind turbine rotor speed (in rad/sec), respectively.The wind turbine mechanical torque output Tm given as:

$$T_m = \frac{1}{2}\rho A C_p(\lambda,\beta)v^3\left(\frac{1}{w_m}\right)$$

A generic equation is used to model the coefficient of power conversion $C_p(\lambda, \beta)$ based on the modelling turbine characteristics described as:

ISSN No: 2348-4845
International Journal & Magazine of Engineering, Technology, Management and Research
A Peer Reviewed Open Access International Journal

$$C_p = \frac{1}{2}\left(\frac{116}{\lambda_i} - 0.4\beta - 5\right)e^{-\left(\frac{21}{\lambda_i}\right)}$$

$$\frac{1}{\lambda_i} = \frac{1}{\lambda + 0.08\beta} - \frac{0.035}{\beta^3 + 1}$$

The coefficient of power conversion and the power are maximums at a certain value of tip speed ratiocalled optimum tip speed ratioλopt. Therefore, the maximum value of C_p(λ, β), that is$max C_p$ = 0.41, is achieved for λopt = 8.1 and for β =0^0. Besides, any change in the wind velocity or the generator speedinduces change in the tip speed ratio leading to power coefficient variation. Consequently, the extracted power is affected.

PMSG modeling

The mathematical model of a PMSG is usually defined in the rotating reference frame d-q as follows

$$v_{gq} = (R_g + p.L_g)i_q + w_e L_d i_d + w_e \psi_f$$

$$v_{gd} = (R_g + p.L_d)i_d + w_e L_q i_q$$

Where$v_{gd}$and $v_{gq}$are the direct stator and quadrature stator voltage, respectively. i_d And $i_q$are thedirect stator and quadrature stator current, respectively. Rg is the stator resistance, Lq and Ldare theinductances of the generator on the q and d axis, ψ_f is the permanent magnetic flux and ω_e is the electrical rotating speed of the generator, defined by:

$\omega_e = \omega_m p_n$

Where p_n is the number of pole pairs of the generator and m ω is the mechanical angular speed.

The electromagnetic torque can be described as:

$$T_e = \frac{3}{2}p_n\left[\psi_f i_q - (L_d - L_q)i_d i_q\right]$$

If i_d = 0, the electromagnetic torque is expressed as

$$T_e = \frac{3}{2}p_n \psi_f i_q$$

The dynamic equation of the wind turbine is described by:

$$J\left(\frac{dw_m}{dt}\right) = T_e - T_m - Fw_m$$

Where J is the moment of inertia, F is the viscous friction coefficient and Tm is the mechanical torque developed by the wind turbine.

Control system of PMSG's VSC

Fig. 2 illustrates the control block diagrams of the indicesm_{q1} and m_{d1} of the studied PMSG's VSC.

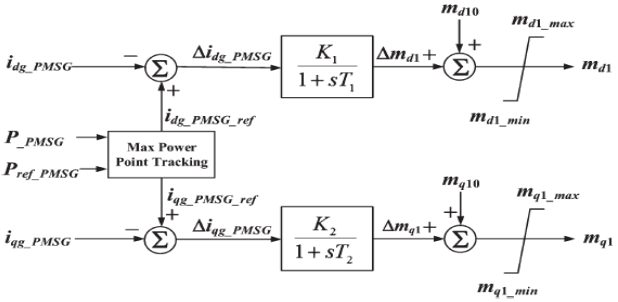

Fig 2: Control block diagram of the modulation indices of the VSC of the studied PMSG.

The d- and q-axis reference currents are generated by comparing the output activepower of the PMSG (P_{PMSG}) with its reference value usingmaximum power point tracking function. After subtracting theoutput currents of the PMSG (i_{g_PMSG}) from their respective reference values, the resultant differences pass through the respectivefirst-order lag controllers to obtain the deviations of therespective modulation indices that are added to their respectiveinitial values to acquire the VSC's modulation indices.

MPPT Algorithm

The MPPT process in the proposed system is based on indirectly adjusting the VSC modulation indices according to the result of the comparison of successive WG-output-power measurements. Thus, the problem of maximizing the WG output power using the converter duty cycle as a control variable can be effectively solved using the steepest ascent method according to the following control law:

$$D_k = D_{k-1} + C_1.\left(\frac{\Delta P_{k-1}}{\Delta D_{k-1}}\right)$$

WhereD_k and D_{k-1} are the duty-cycle values at iterationsk and k − 1, respectively (0 <D_k< 1); $\Delta P_{k-1}/D_{k-1}$is the WG power gradient at step k − 1; and C_1 is the step change.

In order to ensure that this method results in convergence to the WG MPP at any wind-speed level, it is adequate to

ISSN No: 2348-4845
International Journal & Magazine of Engineering, Technology, Management and Research
A Peer Reviewed Open Access International Journal

prove that the function P (D), relating the WG power P and the dc/dc converter duty cycle D, has a single extreme point coinciding with the WG MPPs.

$$\frac{dP}{d\Omega} = 0$$

Where Ω is the WG rotor speed

Applying the chain rule, the above equation can be written as

$$\frac{\mathrm{dP}}{\mathrm{d}\Omega} = \frac{\mathrm{dP}}{\mathrm{dD}} \cdot \frac{\mathrm{dD}}{dV_{WG}} \cdot \frac{dV_{WG}}{d\Omega_e} \cdot \frac{d\Omega_e}{\mathrm{d}\Omega} = 0$$

Where V_{WG} is the rectifier output voltage level and Ωe is the generator-phase-voltage angular speed.

In case of a buck-type dc/dc converter, its input voltageis related to the output (battery) voltage and the duty cycles follows:

$$D = \frac{V_0}{V_{WG}}$$

$$\frac{dD}{dV_{WG}} = -\frac{1}{V_{WG}^2} V_0 \neq 0$$

WhereV_0 is the battery voltage level

The wind-turbine rotor speed is related to the generator speed as follows:

$$\Omega_e = p.\Omega$$

$$\frac{d\Omega_e}{\mathrm{d}\Omega} = p > 0$$

Where p is the generator number of pole pairs

The rectifier output voltage V_{WG} is proportional to the generator phase voltage Vph; it is concluded that

$$\frac{dV_{ph}}{d\Omega_e} > 0$$

And

$$\frac{dV_{WG}}{d\Omega_e} > 0$$

It holds that

$$\frac{\mathrm{dP}}{\mathrm{d}\Omega} = 0 \Leftrightarrow \frac{\mathrm{dP}}{\mathrm{dD}}$$

Thus, the function P (D) has a single extreme point, coinciding with the WG MPP, and the dc/dc converter duty-cycle adjustment according to the control law of (5) ensures convergence to the WG MPP under any wind-speed condition. The power maximization process is shown in Fig. 5. Since the duty-cycle adjustment follows the direction of dP/dD, the modulation indices value is increased in the high-speed side of the WG characteristic, resulting in a WG-rotor-speed reduction and power increase, until the MPP is reached. Similarly when the starting point is in the low-speed side, following the direction of dP/dD results in duty-cycle reduction and the subsequent convergence at the MPP, since the WG rotor speed is progressively increased.

Power Characteristics of the AWS-Based WEC

The AWS-based WEC consists of the AWS and the LPMG. The dynamics of the AWS-based WEC include the mechanical dynamics of the AWS and the electromagnetic dynamics of the LPMG. The dynamic model of the AWS-based WEC is derived as follows. A phasor model for AWS-based WEC was obtained using Park's Transformation, which is suitable for power system dynamic analysis.

Motion Equation of the AWS since the LPMG is driven directly by the AWS, the AWS and the translator of the LPMG can be considered as one-mass. The forces acting on the AWS were analyzed and the detailed motion equation of the AWS was also derived. Based on the motion equation of the AWS, a simplified motion equation is derived which is suitable for power system analysis. The simplified motion equation is given by

$$\frac{dx}{dt} = v$$

$$m_{tot}.\frac{dv}{dt} + \beta_g v + \beta_w v + k_s x = F_{wave}$$

where x is the distance traveled by the floater and the translator; v is the speed of the floater and the translator; m_{tot} is the total mass of the floater, translator of the LPMG, the water above the AWS that has to be accelerated, and various parts moving with the floater; β_g is the damping coefficient of the LPMG; β_w is the hydrodynamic damping coefficient of the AWS; k_s is the spring constant of the AWS; F_{wave} is the sum of the forces acting on the floater resulting from the waves, which is responsible for exciting the dynamics of the AWS.

ISSN No: 2348-4845
International Journal & Magazine of Engineering, Technology, Management and Research
A Peer Reviewed Open Access International Journal

When$v > 0$: Similar to the positive definition of the voltage, flux linkage, and the current of the synchronous generator, the stator flux linkage equation in abc reference frame can be written as

$$\varphi_s = -Li_{abc} + \varphi_{PM_{abc}}$$

where $\varphi_s$is the vector of the stator circuit flux linkage and given by $[\varphi_a \quad \varphi_b \quad \varphi_c]^T$; $i_{abc}$is the vector of the stator current and given by $[i_a \quad i_b \quad i_c]^T$; is the matrix of the inductance; $\varphi_{PM_abc}$is the flux linkages of the stator circuit due to the permanent magnet. L and $\varphi_{PM_abc}$are given by

$$L = \begin{bmatrix} L_{ss} & M & M \\ M & L_{ss} & M \\ M & M & L_{ss} \end{bmatrix}$$

$$\varphi_{PM_{abc}} = \begin{bmatrix} \varphi_{PM} \sin\left(\frac{2\pi}{\lambda}\right) \\ \varphi_{PM} \sin\left(\frac{2\pi x}{\lambda} - \frac{2\pi}{3}\right) \\ \varphi_{PM} \sin\left(\frac{2\pi x}{\lambda} + \frac{2\pi}{3}\right) \end{bmatrix}$$

Where $L_{ss}$is the self-inductance of a phase; M is the mutual inductance between two stator phases, and M<0; λ is the pole width of the LPMG; φ_{PM} is the flux linkage of the permanent magnet. The stator voltage equation in the abc reference frame can be written as

$$u_{s_{abc}} = -Ri_{abc} + \frac{d\varphi_s}{dt}$$

Where $u_{s_abc}$is the vector of the terminal voltage; R=diag $[R_s, R_s, R_s]$, where R_s is the resistance of a phase winding.

The voltage equation can be written as

$$u_{s_{abc}} = -Ri_{abc} + \frac{d\left(-Li_{abc} + \varphi_{PM_{abc}}\right)}{dt}$$

When$v < 0$: Since the direction of the motion of the translator is inversed, the direction induced voltage is accordingly inversed, so is the direction the corresponding current, while the direction of the flux linkage of the permanent magnet is kept. This means the flux linkage reacting to the variation of the flux linkage via the motion of the permanent magnet is generated by the inversed current. Hence, the stator flux linkage equation can be written as

$$\varphi_s = Li_{abc} + \varphi_{PM_{abc}}$$

The voltage equation can be written as

$$u_{s_{abc}} = -Ri_{abc} + \frac{d\left(Li_{abc} + \varphi_{PM_{abc}}\right)}{dt}$$

Model of LPMG in the dq0 Frame of Reference Fixed in the Translator

When$v > 0$: the stator voltage equation of the LPMG in dq reference frame as shown in the following can be derived:

$$u_{ds} = -Ri_{ds} + wL_s i_{qs} - L_s \frac{di_{ds}}{dt}$$

$$u_{qs} = -Ri_{qs} - wL_s i_{ds} - L_s \frac{di_{qs}}{dt} + w\varphi_{PM}$$

And the active power equation is given by

$$P_s = \frac{3}{2} w\varphi i_{qs}$$

where $u_{ds}$and $u_{qs}$are the d-axis and q-axis terminal voltagecomponents of the LPMG, respectively; $i_{ds}$and $i_{ds}$are the d-axis and q-axis stator winding current components of the LMPG,respectively; L_s is the synchronous inductance, w is the angular speed of the stator variables, P_s isthe output active power of the LPMG.

When$v < 0$:

$$u_{ds} = -Ri_{ds} - wL_s i_{qs} + L_s \frac{di_{ds}}{dt}$$

$$u_{qs} = -Ri_{qs} + wL_s i_{ds} + L_s \frac{di_{qs}}{dt} + w\varphi_{PM}$$

The model of the LPMG can be written as

$$L_s . \frac{w}{|w|} \frac{di_{ds}}{dt} = -u_{ds} - Ri_{ds} + X_s i_{qs}$$

$$L_s . \frac{w}{|w|} \frac{di_{qs}}{dt} = -u_{qs} - Ri_{qs} - X_s i_{ds} + +w\varphi_{PM}$$

Where $X_s$is the synchronous reactance, and given by$X_s = |w|L_s$

Since the LPMG is symmetric, the variables of the zero sequence are zero.

Power Equation of the LPMG in the d-q Frame of Reference

The dqframe of reference reciprocates with the translator of AWS. For the sake of illustration, assuming ideal

ISSN No: 2348-4845
International Journal & Magazine of Engineering, Technology, Management and Research
A Peer Reviewed Open Access International Journal

monochromatic waves, the displacement and speed of the floater are given by

$$x = \sin(w_f t)$$
$$v = \cos(w_f t)$$

Where- w_f is the angular speed of the floater.Since the induced voltage is located on the q-axis, and$E_d = 0$, the active power of the LPMG in the dereference frame is given by

$$P = \frac{3}{2} E_q i_q$$

The induced voltage and q-axis component of the stator currentof the LPMG in the dqframe of reference can be written as

$$E_q = \mathrm{E}\cos(w_f t)$$
$$i_q = I_q \cos(w_f t - \varphi)$$

The power of the LPMG can be obtained as follows:

$$P = \frac{3}{2} E I_q \cos(w_f t)\cos(w_f t - \varphi)$$
$$= \frac{3}{2} E I_q (cos^2(w_f t - \varphi) cos\varphi + \cos(w_f t)\sin(w_f t) sin\varphi$$

Above equation describes the instantaneous active power of theLPMG in the frame of reference. Integrating the first term andsecond term of the right-hand side of (above eqn) for one period of themotion of the floater, the following equations can be derived:

$$\int_0^{T_f} \frac{3}{2} E I_q (cos^2(w_f t - \varphi) cos\varphi dt = \frac{3}{2} E I_q T_f \cos(\varphi)$$
$$\int_0^{T_f} \frac{3}{2} E I_q co\,s(w_f t)\, si\,n(w_f t)\, sin\varphi dt = 0$$

Here$T_f$is the period of the motion of the floater. From above eqns, it can be seen that, viewed from the timehorizon of a whole period of the motion of the floater, the firstterm of P demonstrates the characteristics of the active power, while the second demonstrates the characteristics of the reactive power.

Power Equation of the LPMG in the abc Frame of Reference

We have

$$i_q = I_q \cos(w_f t)\cos(\varphi) + I_q \sin(w_f t)\sin(\varphi)$$
$$= i_{q1} + i_{q2}$$

To reduce the power loss in the stator of the LPMG, the axiscomponent of the stator current is normally controlled to zero.

Hence

$$i_d = 0$$

Using the inverse Park's transformation, the induced voltagesand stator currents in the abcframe of reference can be derived as follows:

$$e_a = E\cos(w_f t)\cos\left(\frac{2\pi x}{\lambda}\right)$$
$$e_b = E\cos(w_f t)\cos\left(\frac{2\pi x}{\lambda} - \frac{2\pi}{3}\right)$$
$$e_c = E\cos(w_f t)\cos\left(\frac{2\pi x}{\lambda} - \frac{4\pi}{3}\right)$$
$$i_a = I_q \cos(w_f t)\cos\left(\frac{2\pi x}{\lambda}\right)\cos(\varphi) + I_q \sin(w_f t)\cos\left(\frac{2\pi x}{\lambda}\right)\sin(\varphi)$$
$$i_b = I_q \cos(w_f t)\cos\left(\frac{2\pi x}{\lambda} - \frac{2\pi}{3}\right)\cos(\varphi) + I_q \sin(w_f t)\cos\left(\frac{2\pi x}{\lambda} - \frac{2\pi}{3}\right)\sin(\varphi)$$
$$i_c = I\cos(w_f t)\cos\left(\frac{2\pi x}{\lambda} - \frac{4\pi}{3}\right)\cos(\varphi) + I\sin(w_f t)\cos\left(\frac{2\pi x}{\lambda} - \frac{4\pi}{3}\right)\sin(\varphi)$$

The instantaneous active power in frame of reference isgiven by

$$P_{abc} = i_a e_a + e_b i_b + i_c e_c = \frac{3}{2} i_q E_q$$

Control Blocks of LMSG's VSC

Fig. 3 plots the control block diagrams of the indices $m_{q3}$and m_{d3} of the studied LPMG's VSC. After subtracting theoutput currents of the LPMG (i_{g_LPMG}) from their respectivereference values, the resultant differences pass through therespective proportional-integral controllers to obtain the deviationsof the respective modulation indices which are added totheir respective initial values to obtain the VSC's modulationindices. The limiters,

ISSN No: 2348-4845
International Journal & Magazine of Engineering, Technology, Management and Research
A Peer Reviewed Open Access International Journal

namely,m_{d3_MAX},m_{d3_MIN},m_{q3_MAX}, andm_{q3_MIN}, are included in the model to ensure normal operation of the VSC.

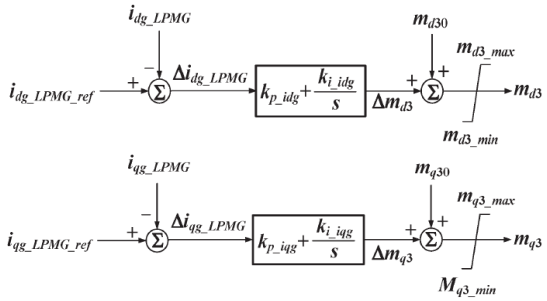

Fig 3: Control block diagram of the modulation indices of the VSC of the studied LPMG

SIMULATION RESULTS

To examine the operation characteristics of the studied integrated system joined with the proposed dc micro grid, the results of the laboratory-grade experimental system and the simulated outcomes using the developed system model are compared. Different experiments are carried out, such as a load switching, speed variations of the wind PMSG, speed variations of the force of the wave LPMG, etc. Only the results under a sudden load-switching condition are shown due to page limit. Fig. 13 shows the responses of the studied system when the connected load is switching from 500 to 1000 W at t = 10 s under the rotor speed of the wind PMSG of 450 r/min and the forcer speed of the wave LPMG of 1.2 m/s. In each subplot shown in Fig. 4, the left one is the measured result, while the right one is the simulated dynamic response, where Park's transformation is used to transform the d–q-axis components into a–b–c three-phase components. For observing the output three-phase voltage or current clearly, only a-phase quantity is shown.

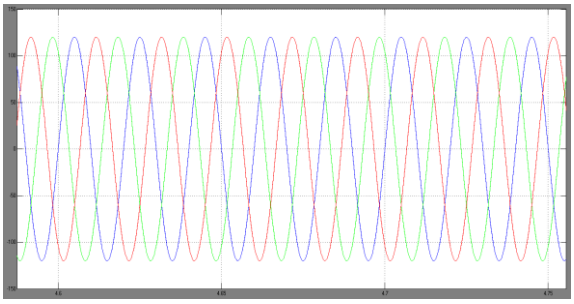

Fig 4(a): Output voltage ofPMSG

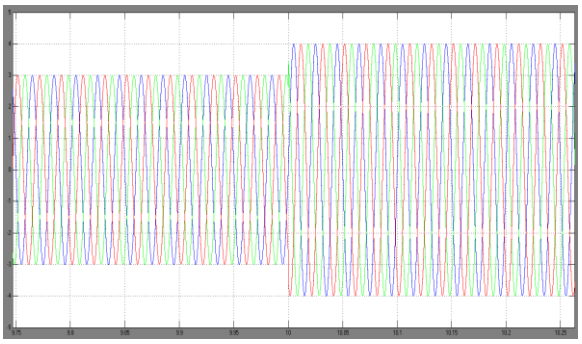

Fig 4(b): Output current of PMSG

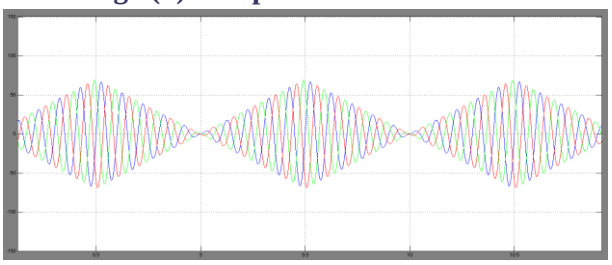

Fig 4(c): Output voltage of the wind LPMG

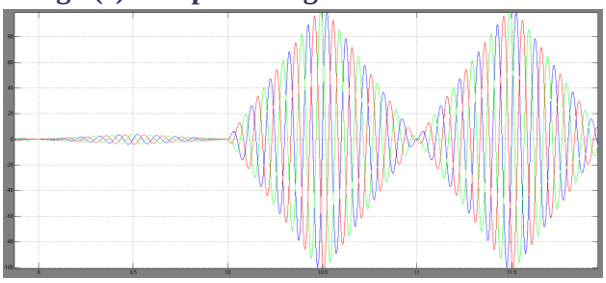

Fig 4(d): Output current of the wave LPMG

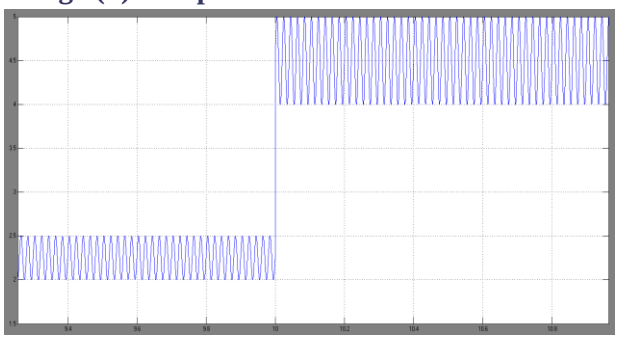

Fig 4(e): Output dc current of the wind PMSG

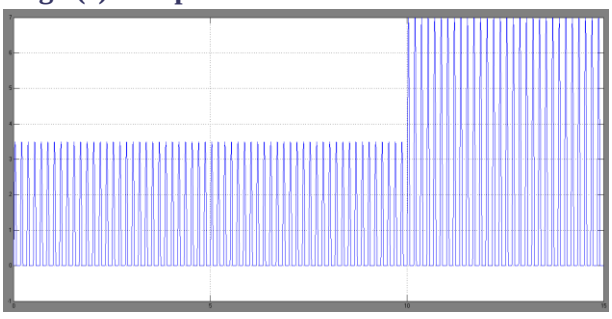

Fig 4(f): Output dc current of the wave LPMG

ISSN No: 2348-4845
International Journal & Magazine of Engineering, Technology, Management and Research
A Peer Reviewed Open Access International Journal

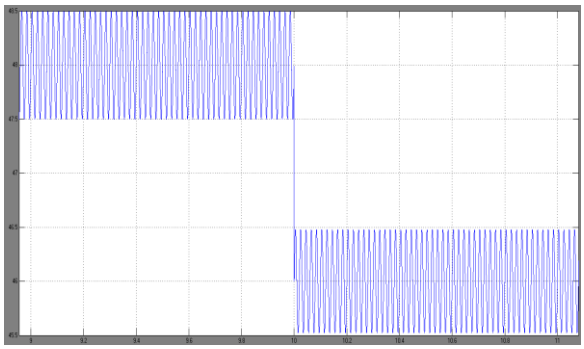

Fig 4(g): DC voltage of the dc micro grid

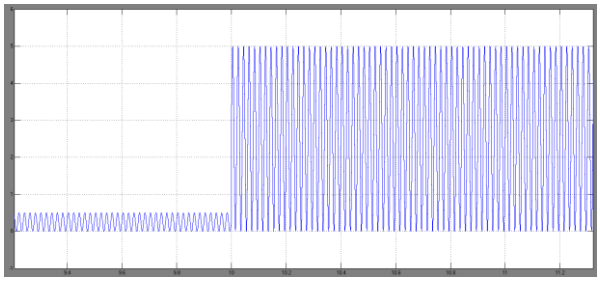

Fig 4(h): Output current of the bidirectional dc/dc converter

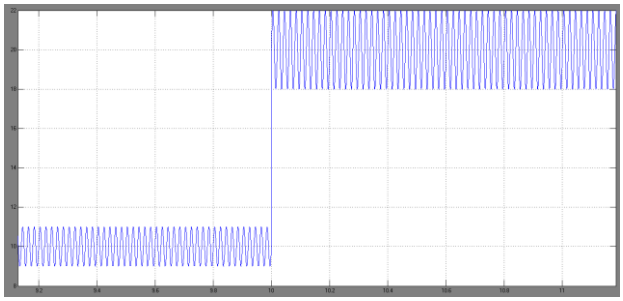

Fig 4(i): DC current flowing into the dc/ac inverter

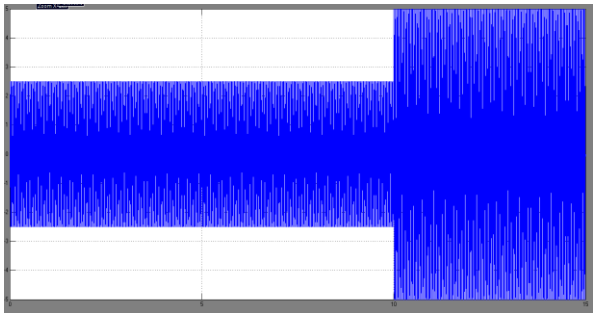

Fig 4(j): Output current of the dc/ac VSI

Integration of hybrid wind/fuel cell based super capacitors distribution Generation Systems to DC Micro grid

Hybrid power systems (HPS) areproposed to overcome these problems with the following twoinnovative improvements.1) Energy storage systems are used to compensate or absorbthe difference between the generated wind power and therequired grid power.2) Power management strategies are implemented to controlthe power exchange among different sources and to providesome services to the grid.Hydrogen technologies, combining fuel cells (FCs) and electrolyzers(ELs) with hydrogen tanks are interesting for longtermenergy storage because of the inherent high mass–energydensity. In the case of wind energy surplus, the EL convertsthe excess energy into H2 by electrochemical reaction. Theproduced H2 can be stored in the hydrogen tank for futurereutilization. In the case of wind energy deficit, the storedelectrolytic H2 can be reused to generate electricity by anFC to meet the energy demand of the grid. Thus, hydrogen, as an energy carrier, contributes directly to the reduction ofdependence on imported fossil fuel.

According to researchers, wind electrolysis is a very attractive candidate foran economically viable renewable hydrogen production system. However, FCs and ELs have low-dynamic performances,and fast-dynamic energy storage should be associatedin order to overcome the fast fluctuations of wind power.Recent progress in technology makes supercapacitors (SCs)the best candidates as fast dynamic energy storage devices,particularly for smoothing fluctuant energy production, likewind energy generators. Compared to batteries, SCs are capableof very fast charges and discharges and can achievea very large number of cycles without degradation, even at100% depth of discharge without “memory effect.” Globally, SCs have a better round-trip efficiency than batteries. Withhigh dynamics and good efficiency, flywheel systems are alsosuitable for fast-dynamic energy storage.

The purpose of this paper is to present the proposed power managementstrategies of the studied HPS order to control the dc-busvoltage and to respect the grid according to the microgrid power requirements. These requirements are formulated as real- andreactive-power references, which are calculated by a centralizedsecondary control center in order to

ISSN No: 2348-4845
International Journal & Magazine of Engineering, Technology, Management and Research
A Peer Reviewed Open Access International Journal

coordinate power dispatchofseveral plants in a control area. This area corresponds to amicrogrid and is limited due to the high level of reliability andspeed required for communications and data transfer.

In this paper, we use a dc-coupled structure in order todecouple the grid voltages and frequencies from other sources.All sources are connected to a main dc bus before beingconnected to the grid through a main inverter.Each source is electrically connected with a power-electronicconverter in order to get possibilities for power control actions.Moreover, this HPS structure and its global control system canalso be used for other combinations of sources.

SIMULATION ANALYSIS

An experimental platform of the HPS has been built to test the different power-balancing strategies. Hardware-In-the-Loop (HIL) emulations of a part of a power system enable a fast experimental validation test before implementation with the real process. Some parts of the simulator process are simulated in real time in a controller board and are then interfaced in hardware with the real devices. Such a HIL simulation has been Intensive ly used and enables one to check the availability and reliability of the hybrid active WG (storage component sizing, power-electronic interface, and operation control).

The FC and EL simulators are used to provide the same electrical behavior as the real FC stack and the EL stack. Models of the FCs and the EL have been previously validated through simulated results from models. Therefore, the equivalent capacitor of the SC bank is about 53 F, and the maximal voltage is about 144 V. All sources are connected to the dc bus through different power converters. The dc bus is connected to the grid through a three-phase inverter, three line filters, and grid transformer. The wind power emulator is used to provide the predefined reduced wind power profile pwg (1.2 kW). The sizing of the FC and EL stacks is adapted by using the modeling parameters of Table II in the IL simulation in order to be interfaced in the experimental test bench. Two power-balancing strategies are tested and compared, respectively. With this experimental test bench, it is possibleto apply our proposed hierarchical control system for the active generator and to test it with the enveloped power-balancing strategies

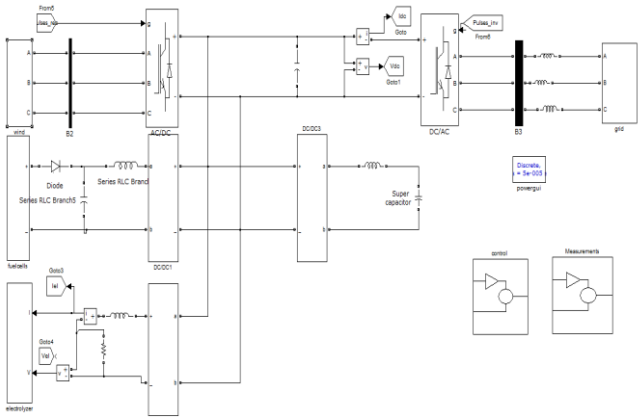

Fig 5: Proposed Novel Hybrid Power System

Power Profile of Different Sources

Two tests are performed experimentally for both strategies, respectively. The same fluctuant wind power profile is usedduring 150 s. The active-power requirement fromthe microgrid is assumed to be *p*gc_ref= 600W. Similar powerprofiles are obtained for the energy storage systems.When the generated wind power is more than 600 W, theEL is activated to absorb the power difference, but when thegenerated wind power is less than 600 W, the FC is activatedto compensate the power difference. Since the power dynamicsof the FCs and the EL are limited by an LPF with a 5-s timeconstant, they are not able to filter the fast fluctuations of thewind power. Therefore, the SCs supply or absorb the power difference.

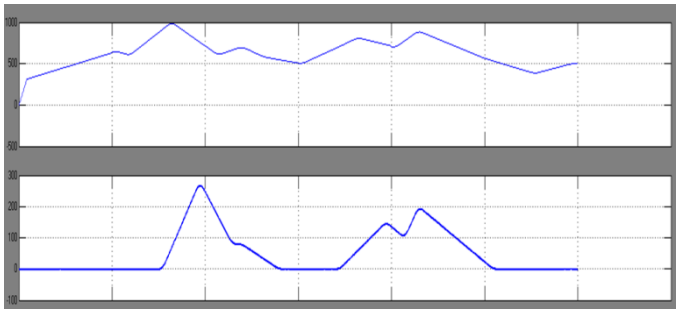

Fig 6: power profiles of wind energy system and super capacitors

ISSN No: 2348-4845
International Journal & Magazine of Engineering, Technology, Management and Research
A Peer Reviewed Open Access International Journal

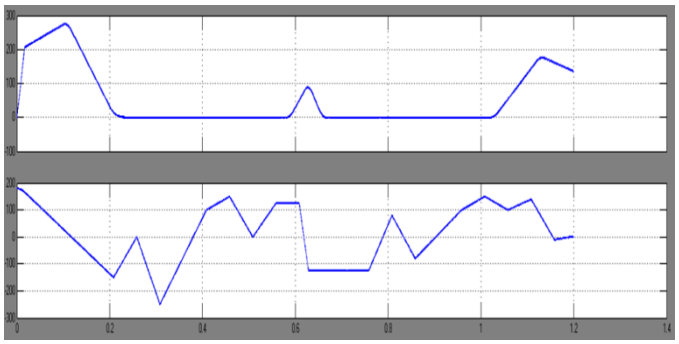

Fig 7: power profiles of fuel energy system and electrolyzer

CONCLUSION

An integration of both wind power and wave power generation systems joined with a dc micro grid has been proposed. A laboratory-grade test system has been presented in this paper to examine the fundamental operating characteristics of the studied integrated system fed to isolated loads using a dc micro grid. For simulation parts, the results of the root-loci plot and the time-domain responses have revealed that the studied integrated system with the proposed dc micro grid can maintain stable operation under a sudden load-switching condition. Comparative simulated and measured results under a load switching have been performed a dc-coupled HPS has been studied with the three kinds of energy sources: 1) a WG as a renewable energy generation system; 2) SCs as a fast-dynamic energy storage system; and 3) FCs with ELs and hydrogen tank as a long term energy storage system. The structure of the control system is divided into three levels: 1) SCU; 2) ACU; and 3) PCU.

Two power-balancing strategies have been presented and compared for the PCU: the grid-following strategy and the source following strategy. For both of them, the dc-bus voltage and the grid power can be well regulated.

REFERENCES

[1] Y. Ito, Y. Zhongqing, and H. Akagi, "DC microgrid based distribution power generation system," in Proc. 4th IEEE Int. Power Electron Motion Control Conf., 2004, vol. 3, pp. 1740–1745.

[2] S. K. Kim, J. H. Jeon, C. H. Cho, J. B. Ahn, and S. H. Kwon, "Dynamic modeling and control of a grid-connected hybrid generation system with versatile power transfer," IEEE Trans. Ind. Electron., vol. 55, no. 4,pp. 1677–1688, Apr. 2008.

[3] C. Abbey and G. Joos, "Super capacitor energy storage for wind energy applications," IEEE Trans. Ind. Appl., vol. 43, no. 3, pp. 769–776, May 2007.

[4] X. Liu, P. Wang, and P. C. Loh, "A hybrid ac/dc micro grid and its coordination control," IEEE Trans. Smart Grid, vol. 2, no. 2, pp. 278–286, Jun. 2011.

[5] H. Kakigano, Y. Miura, and T. Ise, "Low-voltage bipolar-type dc micro grid for super high quality distribution," IEEE Trans. Power Electron., vol. 25, no. 12, pp. 3066–3075, Dec. 2010

[6] M. G. D. S. Prado, F. Gardner, M. Damen, and H. Polinder, "Modeling and test results of the Archimedes wave swing," J. Power Energy, vol. 220,no. 8, pp. 855–868, Dec. 2006.

[7] B. Das and B. C. Pal, "Voltage control performance of AWS connected for grid operation," IEEE Trans. Energy Convers., vol. 21, no. 2, pp. 353–361, Jun. 2006

[8] E. Tara et al., "Dynamic average-value modeling of hybrid-electric vehicular power systems," IEEE Trans. Power Del., vol. 27, no. 1, pp. 430–438,Jan. 2012.

[9] H. L. Do, "Nonisolated bidirectional zero-voltage-switching dc–dc converter," IEEE Trans. Power Electron., vol. 26, no. 9, pp. 2563–2569, Sep. 2011.

[10] D. Salomonsson, L. Söder, and A. Sannino, "An adaptive control system for a dc microgrid for data centers," IEEE Trans. Ind. Appl., vol. 44, no. 6,pp. 1910–1917, Nov./Dec. 2008.

11.M. Lebbal, T. Zhou, B. Francois, and S. Lecoeuche, "Dynamically electrical modelling of electrolyzer and

ISSN No: 2348-4845
International Journal & Magazine of Engineering, Technology, Management and Research
A Peer Reviewed Open Access International Journal

hydrogen production regulation," in Proc. Int. Hydrogen Energy Congr. Exhib., Istanbul, Turkey, Jul. 2007.

[12] R. M. Dell and D. A. J. Rand, "Energy storage—A key technology for global energy sustainability," Power Sources, vol. 100, no. 1/2, pp. 2–17, Nov. 2001